Synthesis and properties of the porous titania coatings formed on titanium by plasma electrolytic oxidation for biomedical application

M. DICU[*], A. MATEI, M. ABRUDEANU, C. DUCU
University of Pitesti, Research Center for Advanced Materials, Targu din Vale, No 1, 110040 Pitesti, Romania

The aim of this study is to explore porous titanium inner-pore wall modification by plasma electrolytic oxidation, with the emphasis on the structural characteristics of the anodized films (including morphology, phase component, element composition and chemical species), and to evaluate the apatite-forming ability of PEO-treated porous titanium in a simulated body fluid (SBF).

1. Introduction

Recently a number of deposition techniques, such as arc-discharge plasma, gas-flame spray, vacuum deposition and high temperature glass enameling, have been investigated to produce layers on light alloys, to increase their wear resistances, corrosion resistance, and so on. However, these techniques require high-energy consumptions to provide adequate layers adhesion under high contact loads.

Therefore, a novel electrochemical surface treatment process, plasma electrolytic oxidation (PEO), was introduced, which could generate ceramic layers on light metals with low energy consumption. [1]

This technique, dated back to 1930s, when Gunterschulze and Betz first studied spark discharge at the anode surface, has been developed quickly in the surface treatment of metals in recent years.

Plasma electrolytic oxidation (PEO) [2], also called micro-arc oxidation (MAO), anodic spark deposition (ASD), or spark anodizing, is a relatively new surface treatment method based on and breaking through the conversional anodic oxidation technology to form ceramic coatings on the so-called valve metals such as aluminum, magnesium, titanium and their alloys in a suitable electrolyte by increasing the anodic voltage to a high stage accompanied by discharge phenomenon.

The PEO technique covers several processes, based on anodisation of a metallic substrate in an electrolyte, with the applied potential sufficiently high for electrical discharges to occur. Among these, the DC PEO mode is the easiest to implement and the most convenient to study fundamental aspects of the coating formation process in relation to the basic process parameters.

PEO usually features plasma discharge phenomena occurring at the metal/electrolyte interface above the breakdown voltage. Discharge events are discrete short-lived and microscopic; they provide multiple heating–cooling cycles to the coating that determine thermal and chemical conditions at the surface, thus playing an important role in the formation of the coating phase composition, structure and stress state.

In the DC PEO mode, discharge characteristics can mainly be controlled by current density [3–5] and electrolyte concentration [2,6,7].

So far, a number of studies had been performed addressing different aspects of the PEO process and the role of effective parameters in the coating process. Thus, some publications deal with fundamentals of the formation mechanism of a coating layer in order to explain possible physical and chemical reactions occurring during the plasma formation [8–13]. Other authors examine the influence of the electrolyte [14–16], the current density [17–19] and the process time [20–22] on the final characteristics of the coatings. Several studies have also been performed to improve the corrosion resistance of the coatings. In this context, various electrolytes were employed in order to obtain high performance coatings [14,15,23,24].

It is reported that various characteristics of these films, e.g. hardness, adhesion, wear resistance and fatigue crack propagation, are influenced by residual stresses which arise mostly during the deposition process [25]. The internal stresses in PEO coatings are caused by: (a) formation and growth of oxide film on the metal surface, (b) thermal effects from surface microdischarges [26,27] and (c) phase transformations in the oxide film.

Stress caused by the formation and growth of oxide film (i.e., intrinsic stress) arises because the oxide usually has a larger volume than that of the metal from which it is formed. If the oxide maintains crystallographic coherency with the underlying metal, then the oxide is compressed, while the metal is extended [28]. Thermal stresses are of different type: (i) stresses caused by differential thermal contraction between coating and substrate and (ii) stresses caused by temperature gradients occurring within the coating during treatment.

However, among the performances of PEO coating, the thermal shock behavior has received less attentions in the past, which is very important in many cases such as the coating used in high temperature environment. So, the thermal shock behavior is now attracting increasing interests [29]. In addition, another very important aspect of PEO coating is the bonding strength between the coating and the substrate, which is the basical for any application of the coating–substrate system. Further more, the few data in literature on thermal shock behavior and bonding strength are mainly concentrated on PEO coating of valve metals such as Al, Ti [30,31]. Researches on these features related to steels still need more attentions.

2. Experimental details

PEO, as a new and effective surface treatment technique developed from traditional anodic oxidation, has been brought for surface modification of many metals, such as Mg, Al, Ti, etc. and alloys [32–36].

Titanium possesses excellent mechanical properties and biocompatibility. Titanium and its thin naturally formed oxide film are known to be bio-inert, therefore, unlike other bioactive materials such as bioglasses and calcium phosphate ceramics, titanium forms osteointegration at the interface of titanium and tissue, instead of bone-bonding.

Titanium and its alloys are widely and successfully used in medicine as implant materials. The longevity of implants (dental implants and orthopedic prostheses) depends on the integration of the implant with the surrounding bone. A very important role in the osteointegration is played by the ability of the surface to form spontaneously hydroxyapatite (HA) in the body fluid. Titanium has many advantageous properties but its ability to form HA on its surface is not as good as that of some ceramics. To improve the osteointegration, the implants are often coated with hydroxyapatite layers.

Various techniques to produce bioactive coatings on titanium have also been explored to improve the bonebonding ability of titanium implants [37–39], among which plasma-sprayed hydroxyapatite (HA) coating is most widely investigated. However, problems of low adhesive strength of the coating to substrate and degradation of the coating were pointed out even in the early stage [40].

Recently, PEO titania film on titanium has been developed in order to enhance the bonding strength of titanium to bone for the rough and porous surface.

After PEO treatment, not only are the rigidity, wear resistance and chemical stability of these metals surprisingly improved [41], but also, the PEO film with a porous structure is favorable for osseous tissue's inward growth of and interconnection with biomaterials, therewith the adhesion of the bone implant / interface is ensured from implantation failure [42,43]. At the same time, bioactive components in the electrolyte such as Ca, P can be incorporated into PEO film during the plasma electrolytic oxidation and thus significantly improve the bioactivity of titanium and titanium alloys [44–48].

The most important feature of PEO is plasma discharge that occurs at the interface between metal and electrolyte when the applied voltage exceeds a critical point. The microstructure and other properties of oxide layer obtained by PEO process depend on the processing conditions, including bath condition, current density, and alloy composition of substrate [48-51]. Especially, corrosion protection capability of oxide layers is highly relied on the chemical composition of electrolyte.

Furthermore, electrolytes used in PEO process are weak alkaline solutions and are friendly to environment. Weak alkaline electrolyte such as silicate, aluminate and phosphate systems are usually used as the base electrolytes [53–56], and in recent years many researchers have tried to improve the properties of PEO coating by adding additives to the electrolyte [52,57–59].

The KOH or NaOH serves to promote electrolytic behaviour (by providing sufficient conductivity) and to adjust the electrolyte pH. Silicates enhance the deposition rate, but can result in porosity and lower coating hardness. Phosphates and other additions contribute to coating hardness and to surface smoothness.

Cooling of the electrolyte is necessary to prolong its useful lifetime. If it is allowed to heat up beyond 30ºC, the coating process can be faster but the electrolyte is depleted of active ingredients much more rapidly.

The choice of the electrolyte is made according to the substrate alloy involved and the desired properties of the coating [60].

To elucidate the current state in this area in the table below we presents a summary of working conditions and types of electrolytes used in several scientific papers. (Table 1).

Table 1. The experimental conditions for getting coatings on titanium by PEO.

Substrate	Working conditions	Electrolyte	Electrolyte Temperature	Ref.
Ti	5-20 Adm^{-2}; 2-10 min; U_o = 450-500 V	$1,0*10^{-1}$ M $Na_2B_4O_7*10H_2O$ $(18,1-90,5)*10^{-3}$ M $Mn(CH_3COO_2)*4H_2O$	13-18°C initial 10-60°C 2-10 min	[61]
Ti	Power source DC 450 V; 100 Hz 1,5;3;5 min	0,20 mol/l $(CH_3COO_2)Ca*H_2O$ 0,04 mol/l $C_3H_7Na_2O_6P*5H_2O$ Immersed in SBF (renewed every 2 days) : 14 and 38 days		[62]
Ti	Power source DC 30 kW; 350 V 200 Hz, 50%, 5 min	0,10 M Na_2 (EDTA); 0,08 CaO; 0,02 M $Ca(H_2PO_4)_2$ Si - incorporated Immersed in SBF 28 days	below 50°C	[63]
Ti	400 V, 50 mA, 1h Hydrothermally heated 220°C-4h	0,02 M calcium β-glycerophosphate 0,15 M calcium acetate Immersed in SBF : 720 and 3000 h	15°C	[64]
Ti	Power source DC 50 mA/cm^2 250–400 V 20 min	Solution A – 0.2 M $Na_2SiO_3 \cdot 5H_2O$+0.04 M calcium β-glycerophosphate (β-GP) Solution B - 0.1M Si $(CH_3COO)_4$+0.04 M Ca-β-glycerophosphate+0.2 M NaOH	15±2 °C	[65]
Ti	Power source DC; 960 s; 435 V; 50 Hz; 20mAcm^{-2}	0.026M Na_3PO_4 pH 12.0; conductivity 7.95mScm^{-1}	20 °C	[66]
Ti	Power source AC; 550 V; 600 Hz; 2, 5, 10, 20 min	0.1 moll^{-1} $(CH_3COO)_2Ca*H_2O$ 0.06 moll^{-1} $NaH_2PO_4*2H_2O$		[67]
Ti	2 A m^{-2} 110 V, 190 V, 340 V	$(NaPO_3)_6$; $CaHPO_4$ pH adjusted to 3.5 with NaOH and H_3PO_4	20 °C.	[68]
Ti	Power source AC 200 mA/cm^2 300 sec	0.02 M KOH and 0.01 M K_3PO_4 pH = 13 Addition of 0.04 M monoclinic zirconia	20 °C	[69]
Ti	250–500V 1000 Hz, 60% and 3 min	0.04 mol/l $(C_3H_7Na_2O_6P * 5H_2O$, b-GP) 0.4 mol/l $(CH_3COO)_2$ Ca * H_2O, CA)		[70]
Ti	Power source DC	calcium glycerophosphate calcium acetate monohydrate		[71]
Ti	Power source DC 240 V to 450 V	An aqueous solution containing calcium salt and phosphate salt		[72]
Ti	Power source AC 50 Hz, 60 kW, 600 V and 100 A	0.1 and 0.2 M NaOH		[73]
Ti	Power source DC 490 V for 1 h – Sample A post treated chemically 1.25 mol NaOH for 12 h- Sample B 400 °C post annealing for 3 h – Sample C	0.04 mol $(NaH_2PO_4 \cdot 2H_2O)$ 0.5 mol NaOH	40 °C	[74]
Ti	10–16 A dm^{-2} 10min 400 v	$(CH_3COO)_2Ca *H_2O$, AR) $(NaH_2PO_4*2H_2O$, AR)	50 °C	[75]
Ti	260–420 V; 60 min 0.5 A/cm^2	0.13 mol/l $(CH_3-COO)_2Ca \cdot H_2O$, AR) 0.06 mol/l $(NaH_2PO_4 \cdot 2H_2O$, AR)	65 °C	[76]

The equipment used for PEO (Fig.1) is similar to that used for conventional anodising, but more complex, primarily due to the need for higher potentials and controlled pulses of current.
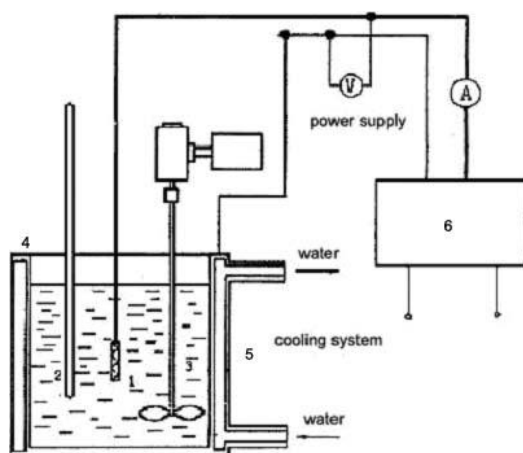
Fig.1. Schematic diagram of the PEO system: (1) Sample (anode); (2) Thermometer; (3) Magnetic stirrer; (4) Cell; (5) Cooling system; (6) Bipolar pulse power supply. [77].

The sample to be coated is cleaned and degreased. It is then electrically connected via an insulated aluminium or titanium jigging arrangement to the copper bus bar, and thus becomes one of the electrodes, immersed in the bath of electrolyte.

The coatings were formed with continuous stirring of the electrolyte in a double-walled glass cell (with a sheet of stainless steel used as the cathode) or stainless steel cell (served as cathode). During the PEO process, the bath was cooled by circulating water. After oxidation process, all of the coated specimens were rinsed thoroughly by distilled water and dried in air.

More complex equipment [78, 79] can provide control of the pulse frequency.

In PEO processes, the anode made by metals is immersed in an aqueous solution, and an asymmetric alternating voltage is applied between the anode and the cathode. In the anodic half circle, the voltage is usually in the range of 150–1000 V, while in the cathodic half circle, the voltage is in the range of 0–100 V. PEO processes are typically characterized by the phenomenon of electrical discharge on the anode in the aqueous solution. A temperature of up to 10,000 K and local pressure of several hundred bars in the discharge channels have been reported.

PEO-treated specimens were examined by Scanning electron microscopy (SEM), X-ray diffraction (XRD), Fourier transform infrared spectroscopy (FT-IR), X-ray photoelectron spectroscopy (XPS) and energy dispersive, X-ray spectrometer (EDX) were utilized for the compositional analyses, etc.

2.2. Immersion of PEO-treated samples in the simulated body fluid

Recently, plasma electrolytic oxidation titania film on titanium has been developed in order to enhance the bonding strength of titanium to bone for the rough and porous surface. Although the titania films containing Ca and P elements [46, 80, 81], they exhibit no bioactivity, because apatite was not formed on the film after the film-coated sample was soaked in the simulated body fluid (SBF)

The ability to promote the deposition of apatite in SBF is well admitted to be a criterion of bioactivity for biomaterials [82, 83].

The PEO coatings were incubated in simulated body fluid (SBF) for several hours to days. The SBF was prepared by dissolving reagent grade chemicals of NaCl, $NaHCO_3$, KCl, $K_2HPO_4 * 3H_2O$, $MgCl_2 * 6H_2O$, $CaCl_2$, and Na_2SO_4 into deionized water at 37 °C.

After immersing for a pre-determined period of time, the samples were removed from the SBF, washed with distilled water and then dried.

3. Results and discussion

Plasma electrolytic oxidation has also been employed in order to modify the surface of titanium and its alloys intended for use as biomaterials, or for improving the mechanical properties of these materials.

The quality of the PEO coating is determined by parameters, such as composition of electrolyte, temperature of electrolyte, alloy composition, voltage, current density, time, etc. High quality coatings can be formed using properly selected deposition parameters.

Ishizawa and Ogino [80, 84, 85] were first to make use of the PEO method for producing hydroxyapatite layers on titanium. They produced the layers using a two-step process: in the first step they enriched the titanium oxide layer with calcium and phosphorus by the PEO method and then transformed the Ca- and P enriched oxide layers into hydroxyapatite using a hydrothermal treatment.

Krupa et al. [65] reported that the PEO treatment increases the corrosion resistance of titanium after 13 h exposure in SBF. Under stationary conditions and during anodic polarization the corrosion resistance of oxidized titanium is higher than that of non-oxidized titanium.

Huang et al. [62] indicated that the surface of titanium plate is rough after the treatment of plasma electrolytic oxidation, and there are many pores of several micrometers in size, which were formed during plasma discharge. Fused mass around the pores is like a volcano top. The temporal temperature of the plasma was very high, which was estimated to be 2000 °C. It seems that the oxidation time had no notable effect on the surface morphology.

The plasma electrolytic oxidation film is composed of rutile TiO_2 and anatase TiO_2 shown in the XRD patterns. The rutile peaks grow higher compared with those of anatase with increasing oxidation time.

Apatite layer was formed on the oxidation film after the sample was immersed in the simulated body fluid for 14 days, and more apatite was deposited at longer immersion time.

The mechanism of apatite formation

The iso-electric points of rutile and anatase are 4.6±0.4 and 5.9±0.2 [86], respectively. They can be negatively charged in SBF (pH=7.40), and absorb Ca^{2+} ions onto the film surface through static electric force. At the same time, Ca^{2+} ions may attract OH^- and $HPO4^{2-}$ groups. Therefore, the supersaturation of SBF to calcium phosphate near the film surface is increased. CaTiO3 finely dispersed in the film can hydrolyze in SBF as follows:

$$CaTiO_3 + 2H_2O \rightarrow Ca^{2+} + 2OH^- + TiO(OH)_2$$
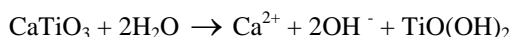
The hydrolysis product $TiO(OH)_2$ is difficult to dissolve [87]. The high concentration of Ti–OH groups was reported to be responsible for apatite formation on sol–gel derived titania film in SBF [88]. Calcium ions released from titania film also increased the ionic activity product of SBF, and provided favorable conditions for apatite nucleation [89].

Once apatite nuclei are formed, they can grow spontaneously by consuming the calcium and phosphate ions in the surrounding fluid, because SBF is highly supersaturated with respect to apatite [89, 90]. Therefore, the plasma electronic oxidation film exhibits bioactivity.

The negatively charging of titania and the hydrolysis of CaTiO3 in SBF contribute to the formation of apatite on the plasma electrolytic oxidation film, and to the possible bioactivity of the oxidation film on titanium.

Zhang et al. [63] reported that it is very significant and promising to incorporate Si into the conventional PEO film by plasma electrolytic oxidation, which can induce certain required elements into the PEO film to enhance its bioactivity and thus to favor skeleton formation. Silicon is believed to be essential in skeleton formation besides calcium and phosphorus. Carlisle [91] first reported in the 1970s that silicon was uniquely localized in the active areas of young bone and involved in the early stage of bone calcification. Schwarz and Milne [92] found that silicon deficiency in rats resulted in skeletal abnormality, especially for cranial bones which appeared flatter than normal. Recently, some Si-containing bioceramics and bioglasses, such as $CaO\text{-}SiO_2$ -based glasses and wollastonite ($CaSiO_3$) ceramics, have been prepared by some researchers [93–95]. These Sicontaining biomaterials were proved to exhibit excellent apatite-induced ability, for example, Liu et al. reported that apatite can be formed completely on the surface of wollastonite ($CaSiO_3$) ceramic after soaking in a SBF solution only for 7 days [96].

It can be seen that the surface morphologies of the two PEO films prepared on Ti substrate in electrolytes with and without silicate are similar, namely, a convex–concave hull-like skeleton with pores is shown on the surface of PEO films. The pores were well separated and distributed homogeneously in the oxide films. But, compared with benchmark PEO film, the average size of micropores in Si-incorporated PEO film was a little bigger. In the new electrolyte, addition of SiO_3^{2-} can enhance the electric conductivity of the electrolyte, which resulted in significant increasing of the partial voltage on the film surface and therefore the instantaneous energy to break open the film locally on sample surface.

Nearly the same peaks were detected for the two specimens, namely, the peaks of rutile TiO_2 and anatase TiO_2 and the peaks of Ti from the substrate. But, the relative intensity of rutile peaks in XRD pattern of the Si - incorporated PEO film is higher than that of benchmark PEO film.

A continuous bone-like apatite layer formation on this film is much faster than on the benchmark film without Si. Compared with the benchmark PEO film, the Si-incorporated PEO film has nearly the same porous structure as well as the same phase constituents, i.e. the two films are consisted of anatase and rutile. However, the Si-incorporated PEO film may be synthesized with high content of new bioactive compounds of CaSiO3 and CaO, which is considered to be the critical factor for the difference in apatite-induced ability of two films.

After immersed into SBF solution, a negative charged surface with abundant functional group ($\equiv Si–O^-$) was created on the surface of the Si-incorporated PEO film, which makes more Ca^{2+} in SBF solution attracted to the interface between film and solution.

Shin et al. [69] reported that the effect of the addition of zirconia particles to the electrolyte on the surface characteristics of the oxide layer on pure titanium subjected to PEO coating was studied.

Zirconium dioxide is a promising coating material, which has high strength, good fracture toughness property, excellent wear resistance and corrosion resistance.

Pores with a size of ~8 μm were observed on the surface in which zirconia particles were uniformly incorporated. This incorporation of zirconia particles caused a significant increase in surface roughness due to the plasma bubbles generated during PEO coating.

Also, uniform occurrence of biomimetic apatite was achieved on the oxide layer having zirconia particles. This was attributed to zirconia particles and high surface roughness responsible for the easy nucleation of biomimetic apatite. Thus, the PEO-coated titanium oxide layer incorporating zirconia particles can be exploited to enhance bioactive properties.

When zirconia particles were added to the electrolyte, the rough surface containing zirconia particles was mainly responsible for promoting the precipitation and even growth of biomimetic apatite. By incorporating zirconia particles into the oxide layer, therefore, the PEO-coated titanium sample exhibits a better bioactive surface with high surface roughness, which would lead to uniform spreading and high proliferation of bone cells.

4. Conclusions

The preparation of the ceramic coatings by bi-polar pulsed PEO technique on Ti and the study on the oxidation behavior of the coated samples under different temperature allowed the following conclusions to be drawn:

- The morphology, chemical composition and thickness of the layers obtained by PEO depend on the electrolyte solution.

- XRD results show that the layers are composed of titanium oxide (anatase and rutile).

- PEO treatment increases the corrosion resistance of titanium after some hours exposure in SBF. Under stationary conditions and during anodic polarization the corrosion resistance of oxidized titanium is higher than that of non-oxidized titanium.

It appeared that the incorporated Ca and P in titania have a similar contribution to the apatite formation. Consequently, it was demonstrated that Ca- and P-containing, micro–arc oxidized titanium implants have the capability to induce bone-like apatite (bioactivity) in the SBF.

The MAO-formed bioactive porous titanium will not only be beneficial to bone ingrowth into the porous structure, but also be beneficial to achieve a tough chemical bonding at the bone/implant interface.

References

[1] G.P. Wirtz, S.D. Brown, W.M. Kriven, Material Manufacture Process **6**, 87 (1991).

[2] A.L. Yerokhin, X. Nie, A. Leyland, A. Matthews, S.J. Dowey, Surf. Coat. Technol. **122**(2–3), 73 (1999).

[3] Y. Guangliang, L. Xianyi, B. Yizhen, C. Haifeng, J. Zengsun, J. Alloy. Compd. **345** (1–2), 196, (2002).

[4] S.G. Xin, Z.H. Jiang, F.P. Wang, X.H. Wu, L.C. Zhao, T. Shimizu, J. Mater. Sci. Technol. **17** (6), 657, (2001).

[5] H.H. Wu, J.B. Wang, B.Y. Long, X.Y. Lu, B.H. Long, Z.S. Jin, Y. Z. Bai, D.M. Bi, Acta Phys. Sin. **54**(12), 5743, (2005).

[6] K. Wang, B.-H. Koo, C.-G. Lee, Y.-J. Kim, S.-H. Lee, E. Byon, Trans. Nonferrous Met. Soc. China **19**(4), 866, (2009).

[7] R.H.U. Khan, PhD, Characteristics and Stress State of Plasma Electrolytic Oxidation Coatings, The University of Sheffield, UK, (2008).

[8] N. Sato, Electrochim. Acta **16,** 1683, (1971).

[9] N.F. Mott, R.J.W. Tobin, Electrochim. Acta **4,** 79 (1961).

[10] L.O. Snizhko, A.L. Yerokhin, A. Pilkington, N.L. Gurevina, D.O. Misnyankin, A. Leyland, A. Matthews, Electrochim. Acta **49,** 2085 (2004).

[11] M.R. Ok, E.Y. Kang, J.H. Kim, Y.S. Ji, C.W. Lee, Y.J. Oh, K.T. Hong, Mater. Sci. Forum **539–543,** 1258, (2007).

[12] M.D. Klapkiv, Mater. Sci. **35,** 279 (1999).

[13] A.G. Rakoch, V.V. Khokhlov, V.A. Bautin, N.A. Lebedeva, Y.V. Magurova, I.V. Bardin, Prot. Met. **42,** 158, (2006).

[14] J. Liang, L. Hu, J. Hao, Appl. Surf. Sci. **253,** 4490 (2007).

[15] H. Duan, C. Yan, F. Wang, Electrochim. Acta **52,** 3785 (2007).

[16] H.Y. Hsiao, H.C. Tsung, W.T. Tsai, Surf. Coat. Technol. **199,** 127 (2005).

[17] Z. Shi, G. Song, A. Atrens, Corros. Sci. **48,** 1939 (2006).

[18] C.B. Wei, X.B. Tian, S.Q. Yang, X.B. Wang, R.K.Y. Fu, P.K. Chu, Surf. Coat. Technol. **201,** 5021 (2007).

[19] S.Y. Chang, Y.L. Kim, B.H. Song, J.H. Lee, Solid State Pheno. **124–126,** 767 (2007)

[20] Y. Ma, X. Nie, D.O. Northwood, H. Hu, Thin Solid Films **494,** 296 (2006).

[21] C. Blawert, V. Heitmann, W. Dietzel, H.M. Nykyforchyn, M.D. Klapkiv, Surf. Coat. Technol. **200,** 68, (2005).

[22] Y. Ma, H. Hu, D. Northwood, X. Nie, J. Mater. Proce. Technol. **182,** 58 (2007).

[23] Q. Cai, L. Wang, B. Wei, Q. Liu, Surf. Coat. Technol. **200,** 3727 (2006).

[24] Y. Ma, X. Nie, D.O. Northwood, H. Hu, Thin Solid Films **469–470,** 472 (2004).

[25] E. Atar, C. Sarioglu, U. Demirler, E.S. Kayali, H. Cimenoglu, Residual Stress Estimation of Ceramic Thin Films by X-ray Diffraction and Indentation Techniques, Elsevier, (2003).

[26] A.L. Yerokhin, X. Nie, A. Leyland, A. Matthews, S.J. Dowey, Surf. Coat. Technol. **122,** 2, (1999).

[27] A.L. Yerokhin, L.O. Snizhko, N.L. Gurevina, A. Leyland, A. Pilkington, A. Matthews, J. Appl. Phys. **36,** 2110, (2003).

[28] Society for Automotive Engineering, Residual Stress Measurement by X-ray Diffraction, 2nd edR, SAE, p. J748a, (1971).

[29] J.A. Curran, T.W. Clyne, Surf. Coat. Technol. **199,** 168–176 (2005).

[30] D.J. Shen, Y.L. Wang, P. Nash, G.Z. Xing, J. Mater. Process. Technol. **205,** 477–481, (2008).

[31] Y.M. Wang, L.X. Guo, J.H. yang, Y. Zhou, D.C. Jia, Appl. Surf. Sci. **255,** 6875–6880, (2009).

[32] H.X. Li, V.S. Rudnev, X.H. Zheng, T.P. Yarovaya, R.G. Song, J. Alloys Compd. **462,** 99–102, (2008).

[33] H.P. Duan, C.W. Yan, F.H.Wang, Electrochim. Acta **52,** 5002–5009 (2007).

[34] W.C. Gu, G.H. Lv, H. Chen, G.L. Chen, W.R. Feng, G.L. Zhang, S.Z. Yang, J. Alloys Compd. **430,** 308–312, (2007).

[35] L.O. Snizhko, A.L. Yerokhin, A. Pilkington, et al., Electrochim. Acta **49,** 2085–2095, (2004).

[36] J.L. Xu, F. Liu, F.P.Wang, D.Z. Yu, L.C. Zhao, J. Alloys Compd. **472,** 276–280, (2009).

[37] L. Ellies, D. Nelson, J. Featherstone, Biomaterials **13,** 313, (1992).

[38] R. Whitehead, W. Lacefield, L. Lucas, J. Biomed. Mater. Res. **27,** 1501, (1993).

[39] H. Ji, P. Marquis, Biomaterials **14**, 64, (1993).

[40] Z. Zyman, J. Weng, X. Liu, X. Li, X. Zhang, Biomaterials **15,** 151, (1994).

[41] W. Xue, C. Wang, R. Chen, Z. Deng, Mater. Lett. **52,** 435, (2002).

[42] M. Svehla, P. Morberg, B. Zicat, et al. J. Biomed. Mater. Res. **51,** 15, (2000).

[43] B. Chehroudi, D.D. Mc, D.M. Brunette, J. Biomed. Mater. Res. **34,** 279, (1997).

[44] Y. Han, S.-H. Hong, K.W. Xu, Surf. Coat. Technol. **168,** 249, (2003).

[45] H. Ishizawa, M. Fujino, M. Ogino, J. Biomed. Mater. Res. **29,** 1459, (1995).

[46] H. Ishizawa, M. Ogino, J. Biomed. Mater. Res. **29,** 1071, (1995),

[47] H. Ishizawa, M. Ogino, J. Biomed. Mater. Res. **29,** 65, (1997).

[48] W.-H. Song, Y.-K. Jun, Y. Han, S.-H. Hong, Biomaterials **25,** 3341, (2004)**.**

[49] J. Liang, B. Guo, J. Tian, H. Liu, J. Zhou, W. Liu, T. Xu, [J]. Surf Coat Technol, , **199**, 121-126, (2005).

[50] H. Y. Hsiao, H. C. Tsung, W. T. Tsai, [J]. Surf Coat Technol, **199**, 127-134, (2005).

[51] Z. Shi, G. Song, A. Atrens, [J]. Corros Sci, **48**, 1939-1959, (2006).

[52] J. Liang, B.G. Guo, J. Tian, H.W. Liu, J.F. Zhou, T. Xu, Appl. Surf. Sci. **252,** 345, (2005).

[53] F. Mécuson, T. Czerwiec, T. Belmonte, L. Dujardin, A. Viola, G. Henrion, Surf. Coat. Technol. **200,** 804, (2005).

[54] X.T. Sun, Z.H. Jiang, S.G. Xin, Z.P. Yao, Thin Solid Films **471,** 194, (2005).

[55] B.H. Long, H.H. Wu, B.Y. Long, J.B. Wang, N.D. Wang, X.Y. Lü, Z.S. Jin, Y.Z. Bai, J. Phys. D Appl. Phys. **38,** 3491, (2005).

[56] G. Lv, W. Gu, H. Chen, W. Feng, M.L. Khosa, L. Li, E. Niu, G. Zhang, S.Z. Yang, Appl. Surf. Sci. **253,** 2947, (2006).

[57] H. Duan, C. Yan, F. Wang, Electrochim. Acta **52,** 3785, (2007).

[58] F. Jin, P.K. Chu, H.H. Tong, J. Zhao, Appl. Surf. Sci. **253,** 863, (2006).

[59] G.H. Lv, H. Chen, W.C. Gu, W.R. Feng, L. Li, E.W. Niu, X.H. Zhang, S.Z. Yang, Curr. Appl. Phys. **9**, 324, (2009).

[60] J.A. Curran, Ph.D Thesis, Peterhouse College, University of Cambridge, Cambridge, United Kingdom, (2005).

[61] V.S. Rudnev, M.S. Vasilyeva, N.B. Kondrikov, L.M. Tyrina, Applied Surface Science **252,** 1211–1220, (2005).

[62] P. Huang, Ke-W. Xu, Y. Han, Materials Letters **59,** 185– 189, (2005).

[63] W. Zhang, D. Keqin, Y. Chuanwei, F. Wang, Appl. Surf. Sci. **254,** 5216–5223, (2008).

[64] J. Baszkiewicz, D. Krupa, J. Mizera, J.W. Sobczak, A. Bilin´ski, Vacuum **78,** 143–147, (2005).

[65] D. Krupa, J. Baszkiewicz, J. Zdunek, J. Smolik, Z. Słomka, J. W. Sobczak, Surface & Coatings Technology **205** (6), 1743-1749, (2010).

[66] E. Matykina, A. Berkani, P. Skeldon, G.E. Thompson, Electrochimica Acta **53,** 1987–1994, (2007),

[67] Z.Q. Yao, Yu. Ivanisenko, T. Diemant, A. Caron, A. Chuvilin, J.Z. Jiang, R.Z. Valiev, M. Qi, H.-J. Fecht, Acta Biomaterialia **6,** 2816–2825, (2010).

[68] E. Matykina, R. Arrabal, P. Skeldon, G.E. Thompson, Acta Biomaterialia **5,** 1356–1366, (2009),

[69] K. R. Shin, Y. G. Ko, D. H. Shin, Materials Letters **64** (24), 2714-2717, (2010).

[70] Won-H. Song, Youn-K. Jun, Y. Han, Seong-H. Hong, Biomaterials **25,** 3341–3349, (2004).

[71] F. Liu, Y. Song, F. Wang, T. Shimizu, K. Igarashi, L. Zhao, Journal of Bioscience and Bioengineering **100** (1), 100–104, (2005).

[72] P. Huang, F. Wang, K. Xu, Y. Han, Surface & Coatings Technology, **201,** 5168–5171, (2007).

[73] J. Sun, Y. Han, K. Cui, Surface & Coatings Technology **202,** 4248–4256, (2008).

[74] Po-J. Chu, Shu-Y. Wu, Keh-C. Chen, Ju-L. He, A. Yerokhin, A. Matthews, Thin Solid Films **519**(5), 1723 (2010).

[75] Jia-H. Ni, Yu-L. Shi, Feng-Y. Yan, Jian-Z. Chen, L. Wang, Materials Research Bulletin **43,** 45 (2008).

[76] Jian-zhi Chen, Yu-long Shi, L. Wang, Feng-ying Yan, Fu-qiang Zhang, Materials Letters **60,** 2538 (2006).

[77] Y. Wang, Z. Jiang, Z. Yao, Current Applied Physics **9,** 1067 (2009),

[78] A.S. Shatrov, V.I. Samsonov, GB Patent 2 386 907 Forming ceramic coatings on metals and alloy (2003): GB.

[79] A.S. Shatrov, and V.I. Samsonov, Patent WO 03/083181 A2 Process and device for forming ceramic coatings on metals and alloys, and coatings produced by this process. (2003): World Intellectual Property Organisation.

[80] H. Ishizawa, M. Ogino, J. Biomed. Mater. Res. **29,** 65 (1995).

[81] H. Ishizawa, M. Ogini, J. Biomed. Mater. Res. **29,** 1459, (1995).

[82] T. Kitsugi, T. Nakamura, T. Tamamuro, J. Kokubo, Biomed. Mater. Res. **21,** 1255 (1987).

[83] M. Neo, S. Kotani, T. Nakamura, T. Yamamuro, C. Ohtsuki, T. Kokubo, Y. Bando, J. Biomed. Mater. Res. **26** (11), 1419, (1992).

[84] H. Ishizawa, M. Ogino, J. Biomed. Mater. Res. **29,** 1071 (1995).

[85] H. Ishizawa, M. Fujino, M. Ogino, J. Biomed. Mater. Res. **29,** 1459 (1995).

[86] T. Hanawa, M. Kon, H. Doi, J. Mater. Sci., Mater. Med. **9**, 89, (1998).

[87] M.T. Pham, W. Matz, H. Reuther, Surf. Coat. Technol. **128–129**, 313, (2000).

[88] T. Kokuto, F. Miyaji, H.M. Kim, T. Nakamura, J. Am. Ceram. Soc. **79,** 1127, (1996).

[89] T. Kokubo, H. Kim, M. Kawashita, Biomaterials **24,** 2161 (2003).

[90] W. Neuman, M. Neuman, The Chemical Dynamics Of Bone Mineral, University of Chicago Press,

Chicago, IL, (1958).
[91] E.M. Carlisle, Science **167,** 279, (1970).
[92] K. Schwarz, D.B. Milne, Nature **239,** 333, (1972).
[93] K. Ono, T. Yamamuro, T. Nakamura, T. Kokubot, Biomaterials **11,** 265 (1990).

[94] P.N. De Aza, Z.B. Luklinska, M.R. Anseau, M. Hector, F. Guitia´n, S. De Aza, Biomaterials **21**, 1735 (2000).
[95] T. Kokubo, J. Non-Cryst. Solids **120,** 138, (1990).
[96] X.Y. Liu, C.X. Ding, Z.Y. Wang, Biomaterials **22,** 2007 (2001).

_____

*Corresponding author: ela_magda@yahoo.com